Plant Mol Biol (2017) 93:419–429
DOI 10.1007/s11103-016-0570-8

Formation of wood secondary cell wall may involve two type cellulose synthase complexes in *Populus*

Wang Xi[1] · Dongliang Song[1] · Jiayan Sun[1] · Junhui Shen[1] · Laigeng Li[1]

Received: 29 March 2016 / Accepted: 2 December 2016 / Published online: 16 December 2016

Abstract Cellulose biosynthesis is mediated by cellulose synthases (CesAs), which constitute into rosette-like cellulose synthase complexe (CSC) on the plasma membrane. Two types of CSCs in *Arabidopsis* are believed to be involved in cellulose synthesis in the primary cell wall and secondary cell walls, respectively. In this work, we found that the two type CSCs participated cellulose biosynthesis in differentiating xylem cells undergoing secondary cell wall thickening in *Populus*. During the cell wall thickening process, expression of one type CSC genes increased while expression of the other type CSC genes decreased. Suppression of different type CSC genes both affected the wall-thickening and disrupted the multilaminar structure of the secondary cell walls. When *CesA7A* was suppressed, crystalline cellulose content was reduced, which, however, showed an increase when *CesA3D* was suppressed. The *CesA* suppression also affected cellulose digestibility of the wood cell walls. The results suggest that two type CSCs are involved in coordinating the cellulose biosynthesis in formation of the multilaminar structure in *Populus* wood secondary cell walls.

W. Xi and D. Song have contributed equally to this work.

Electronic supplementary material The online version of this article (doi:10.1007/s11103-016-0570-8) contains supplementary material, which is available to authorized users.

✉ Laigeng Li
lgli@sibs.ac.cn

[1] National Key Laboratory of Plant Molecular Genetics, CAS Center for Excellence in Molecular Plant Sciences, Institute of Plant Physiology and Ecology, Chinese Academy of Sciences, Shanghai 200032, China

Keywords Cellulose synthase · Secondary cell wall · Wood formation · *Populus*

Introduction

Cellulose, the most abundant biopolymer on Earth, is accumulated in the plant cell walls which is a major resource for pulping, biomaterial and lignocellulosic biofuel production. Wood tissue in trees mainly consists of the secondary cell walls, containing 42–50% cellulose (Sjöström 1993). Usually wood secondary cell walls can be divided into three layers, S1, S2 and S3, which differ with respect to the cellulose content, degree of polymerization (DP), microfibril crystallinity and orientation (Buchanan et al. 2000; Sjöström 1993; Mellerowicz and Sundberg 2008; Washusen and Evans 2001; Müller et al. 2006). However, the mechanisms underlying formation of the multilaminar secondary cell walls structured with different cellulose characters remains unclear.

Celluloses in primary and secondary cell walls also display different characteristics such as microfibril crystallinity and DP (Blaschek et al. 1982; Sjöström 1993; Buchanan et al. 2000; Mellerowicz and Sundberg 2008; Müller et al. 2006; Washusen and Evans 2001). Cellulose synthesized in primary cell wall contains low degree of microfibril crystallinity and low DP. In contrast, the thick secondary cell walls contain cellulose with high crystallinity and high DP. In higher plants, cellulose is synthesized on the plasma membrane by cellulose synthase complexe (CSC) (McFarlane et al. 2014; Somerville 2006). The plant CSC, which has been visualized as a six-lobed rosette structure, is comprised of six subunits which are composed of 6 cellulose synthase (CesA) proteins (Somerville 2006; Doblin et al. 2002; Mutwil et al. 2008; Delmer 1999; Kimura

et al. 1999). Thus, it is suggested that 36 CesA proteins are organized in a CSC and simultaneously contributed to the formation of one elementary microfibril in plant cell walls (Somerville 2006; Doblin et al. 2002; Saxena and Brown 2005). Nevertheless, multidimensional solid-state NMR analysis indicated that the primary-wall cellulose microfibrils contain at least 24 glucan chains (Wang and Hong 2016), while another study reported that CSC is composed of a hexamer of catalytically active CESA trimers, which may result in producing 18-chain cellulose microfibrils (Hill et al. 2014). The exact number of CesAs in a CSC is yet to be determined.

In *Arabidopsis*, celluloses in primary and secondary walls are reported to be synthesized by different CesA proteins which assemble into different CSCs (Desprez et al. 2007; Atanassov et al. 2009; McFarlane et al. 2014). Genetic evidence showed that both CesA1 and CesA3 protein are necessary for primary cell wall cellulose biosynthesis during plant development (Persson et al. 2007; Arioli et al. 1998; Desprez et al. 2007). Biochemical analysis indicated that CesA1, CesA3, and CesA6 interact with each other and form a large complex (840 kDa) (Carroll et al. 2012; Desprez et al. 2007; Wang et al. 2008). During secondary cell wall formation, three other CesA proteins CesA4, CesA7 and CesA8 are found to be integrated into a CSC through a sequential oligomerization process (Atanassov et al. 2009) and each of the three CesA proteins was found to be essential for secondary cell wall cellulose biosynthesis (Taylor et al. 1999, 2000, 2003; Zhong et al. 2003).

However, other studies showed that primary cell wall *CesA* genes are also expressed in cells undergoing secondary cell wall thickening. In *Arabidopsis* shoot trichome cells where the secondary cell wall is thickening, *CesA* genes, including *AtCesA1, 2, 3, 5* and *6* were highly expressed, but *AtCesA4, 7* and *8* were not expressed (Betancur et al. 2010). In epidermal testa cells, *AtCesA9* was also found to play a non-redundant role during secondary cell wall synthesis (Stork et al. 2010). Another study showed that *AtCesA1* could partially rescue the defects in secondary cell wall biosynthesis in *cesa8* mutants, and *AtCesA7* could partially rescue the defects in primary cell wall biosynthesis in *cesa3* mutants, proposing a possibility that CSCs with mixed primary and secondary CesAs could function at particular times when they are co-expressed (Carroll et al. 2012). In *Populus*, transcripts from more than 12 *CesA* genes were detected in differentiating xylem which is undergoing strong secondary cell wall thickening (Suzuki et al. 2006). Furthermore, two type CSCs were biochemically isolated from differentiating xylem tissue (Song et al. 2010). These findings raise a possibility that two type CSCs may simultaneously contribute to the cellulose biosynthesis in wood secondary cell walls.

In this study, we examined the function of two type CSC genes in cellulose biosynthesis during wood secondary cell wall formation. Suppression of each type of *CesA* genes resulted in alterations in wood cellulose content, suggesting that two type CSCs are simultaneously involved in the cellulose biosynthesis of wood secondary cell walls. On the other hand, suppression of two type CSC genes displayed different effect on the crystalline cellulose content and secondary cell wall laminar structure. The results portray a new possibility that two type CSCs coordinates cellulose synthesis in association with formation of the multilaminar structure of wood secondary cell walls in *Populus*.

Results

Expression of two type CSC *CesA*s during secondary cell wall formation

In our previous study, a number of *CesA* genes, including *PtrCesA4, PtrCesA7A, PtrCesA7B, PtrCesA8A, PtrCesA8B, PtrCesA1A, PtrCesA1B, PtrCesA3C, PtrCesA3D, PtrCesA6A* and *PtrCesA6B* were detected for their expression in differentiating secondary xylem tissue (Song et al. 2010). Based on the sequence homology to *Arabidopsis CesA*s, these secondary xylem expressed *Populus CesA*s can be classified to primary cell wall *CesA*s and secondary cell wall *CesA*s. In this study, we further analyzed the two type *CesA* expression in the process of wood secondary cell wall thickening.

During secondary xylem differentiation, secondary cell wall thickening occurs gradually from newly differentiated xylem cells inward to the 10th–12th layer cells in a file of xylem fibers in *Populus*. Following the cell wall thickening process, the differentiating xylem tissue was divided into three wall-thickening stages and collected using laser microdissection (Fig. 1 a–d). *CesA* gene expression was examined in the xylem cells undergoing secondary cell wall thickening. *PtrCesA7A* and *PtrCesA8A* expression significantly inceased during the wall-thickening process (Fig. 2e). In contrast, expression of *PtrCesA1A* and *PtrCesA3D*, belonging to another type CSC genes, gradually decreased during the same process (Fig. 2f). These results indicated that two type *CesA* genes display different expression patterns during the secondary cell wall thickening in wood secondary xylem.

Expression of the two type *CesA* genes was also investigated in field trees. When the trunk from a 5-year-old *Populus* tree in a growth season was debarked, differentiating xylem tissue was separated into early and late stage in wood secondary cell wall thickening. Consistent with the results determined from the microdissected cells, expression of *PtrCesA7A* and *PtrCesA8A* was higher at the late

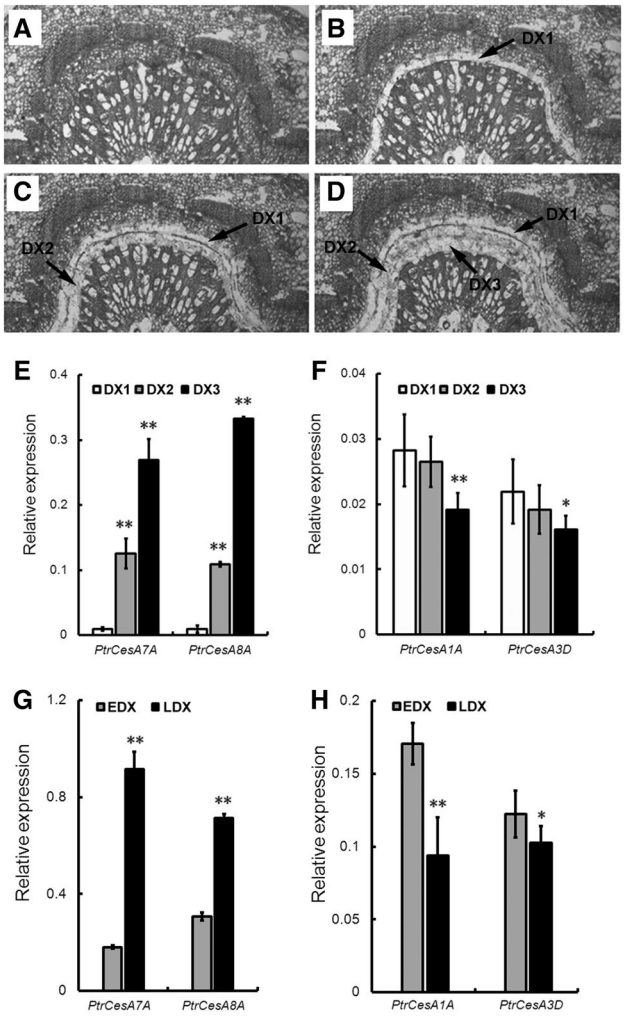

Fig. 1 Two type CSC *CesA*s are differently expressed during secondary cell wall thickening. **a–d** Laser microdissection of differentiating xylem DX1 (including the 1st to 3rd layer xylem cells, possibly mixed with some cambium cells), DX2 (including the 4th to 8th layer cells) and DX3 (including the 9th–12th layer cells). **e** Relative expression of *PtrCesA7A* and *PtrCesA8A* in differentiating xylem cells. **f** Relative expression of *PtrCesA1A* and *PtrCesA3D* in differentiating xylem cells. **g** Expression of *PtrCesA7A* and *PtrCesA8A* in early stage of the differentiating xylem (EDX) and late stage of the differentiating xylem (LDX). **h** Expression of *PtrCesA1A* and *PtrCesA3D* in EDX and LDX. *PtrActin2* was used as a reference gene. Gene expression was measured from three biological repeats. Significance as determined by Student's *t* test. The values are means ± SE. n = 5. **P < 0.01, *P < 0.05

stage than that at the early stage, while expression of *PtrCesA1A* and *PtrCesA3D* was slightly lower at the late stage (Fig. 2g, h).

In addition, presence of CSCs was examined in differentiating xylem using four specific antibodies which can recognize CesA7A/7B and CesA8A/8B in one type CSC, CesA1A/1B and CesA3C/3D in the other type CSC, respectively (Song et al. 2010). The microsomal fraction protein was isolated from the wall-thickening xylem cells and then separated using two-dimensional (2D) Blue Native/SDS gel electrophoresis. The CSCs recognized by four specific antibodies showed a molecular size of more than 669 kDa (Figure S1). Detection of the two type complexes in the wall-thickening xylem cells further verified the involvement of two type CSCs in the secondary cell wall thickening in *Populus*. Together, the results suggest that two type CSCs participate in the wood secondary cell wall thickening.

Suppression of *PtrCesA3D* and *PtrCesA7A* affected *Populus* growth and wood stem mechanic property

To investigate how the two type CSCs participate in cellulose synthesis during wood secondary wall thickening, four CesA genes from the two type CSCs (*PtrCesA7A* and *PtrCesA8A* belonging to one type CSC and *PtrCesA3D* and *PtrCesA1A* belonging to the other type CSC) were specifically suppressed through RNA interference (RNAi). The gene-specific sequences from a CesA hypervariable region (HVR) were constructed into an RNAi vector and transformed into *Populus* by *Agrobacterium*-mediated transformation according to a previous established protocol (Li et al. 2003). The transgenic plants with suppression of *PtrCesA7A* and *PtrCesA8A* expression displayed similar phenotypes, while the transgenics with suppression of *PtrCesA3D* and *PtrCesA1A* expression grew similarly (Figure S2). For detailed analysis, 36 and 42 independent transgenic lines from the *PtrCesA7A* and *PtrCesA3D* suppressions were generated, respectively. After analysis of the transgenic plants, two lines with similar phenotypes (*PtrCesA3Dsp*-L8 and *PtrCesA3Dsp*-L13) from the *PtrCesA3D* suppressed transgenics and two lines (*PtrCesA7Dsp*-L10 and *PtrCesA7Dsp*-L21) from *PtrCesA7D* suppressed transgenics were selected and then multiplied through cutting propagation to create biological repeats for further characterization (Fig. 2). In *PtrCesA3D*-suppressed plants, expression of *PtrCesA3C* and *PtrCesA3D* was down-regulated, but expression of *PtrCesA1A* was not affected (Fig. 2b). While in *PtrCesA7A*-suppressed plants, *PtrCesA7A* and *PtrCesA7B* expression was down-regulated but expression of *PtrCesA8A* was not affected (Fig. 2c). Meanwhile, the PtrCesA3D and PtrCesA7A protein was examined in differentiating xylem tissue and results showed that the amount of PtrCesA3D and PtrCesA7A protein was significantly reduced in their respective suppression transgenics (Fig. 2d). These results indicated that the *CesA* RNAi transformation caused a specific suppression of the target gene expression. Next, we recorded the growth and morphology during a growth season. While the height of the *PtrCesA3D*-suppressed plants (five cutting repeats) was

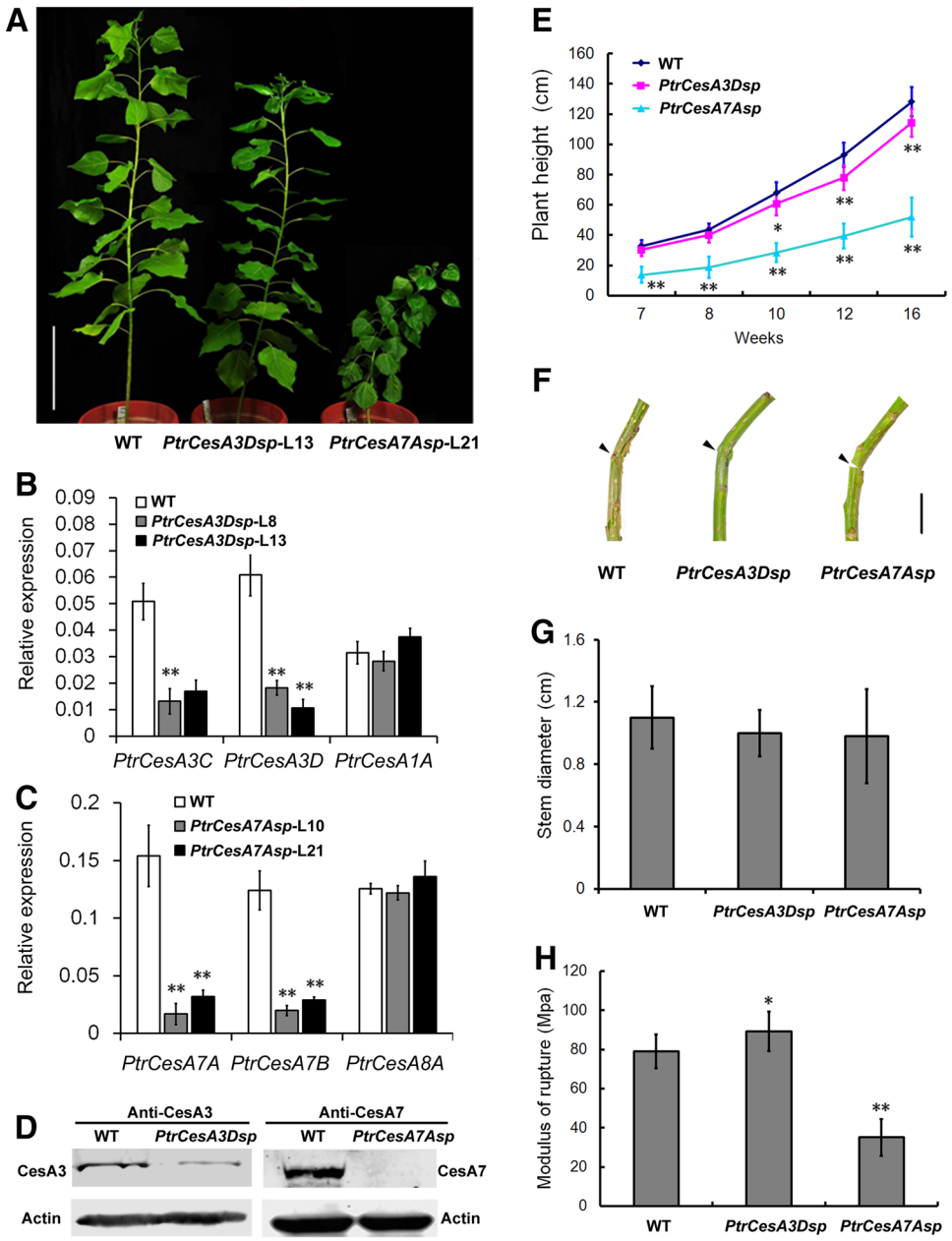

Fig. 2 Characterization of the *CesA* suppressed plants. **a** Morphology of the *Populus* trees grown for 8 months in a green house. *Bar* 15 cm. **b** Expression of *PtrCesA3C, PtrCesA3D* and *PtrCesA1A* in the *PtrCesA3D*-suppressed plants. **c** Expression of *PtrCesA7A, PtrCesA7B* and *PtrCesA8A* in the *PtrCesA7A*-suppressed plants. **d** CesA3 and CesA7 proteins were examined in the transgenic plants. **e** Plant height. **f** Stem of the *PtrCesA7A*-suppressed plants is easier to break, *Bar* 2 cm. **g** Stem diameters. **h** Modulus of rupture of 8-month-old stems. Each transgenic line was multiplied through cutting propagation for biological repeats. Significance as determined by Student's *t* test. The values are means ± SE. n = 5. **P < 0.01, *P < 0.05. *L* Line, *WT* wild-type plants

slightly lower than that of the wild-type plants, the height of *PtrCesA7A*-suppressed plants (five cutting repeats) was dramatically reduced (Fig. 2e). In addition, the stems of the *PtrCesA7A*-suppressed plants were much easier to break, though the stem diameter of the two type transgenic plants did not show significant differences (Fig. 2f, g). The mechanical strength of the stem was reduced in *PtrCesA7A*-suppressed plants, but slightly increased in *PtrCesA3D*-suppressed plants (Fig. 2h). These results indicate that suppression of two different type *CesA* genes had distinct effects on *Populus* growth and stem mechanical property, which could be attributed to the alteration of wood cell walls in the transgenic plants.

Suppression of *PtrCesA3D* and *PtrCesA7A* affected wood secondary cell wall thickening

In order to understand how *CesA* is involved in wall-thickening, we employed a file of fiber cells in *Populus* differentiating xylem to monitor the process of secondary cell wall thickening. During tree growth, vascular cambium division produces a lineage of fiber cells arranged in a file. The wall-thickening process can be sequentially observed in a file of fiber cells using a transmission electron microscope (TEM) (Fig. 3). Under our controlled experimental growth conditions, secondary cell wall thickening in fibers took about 7–10 days to complete. In a fiber file, formation

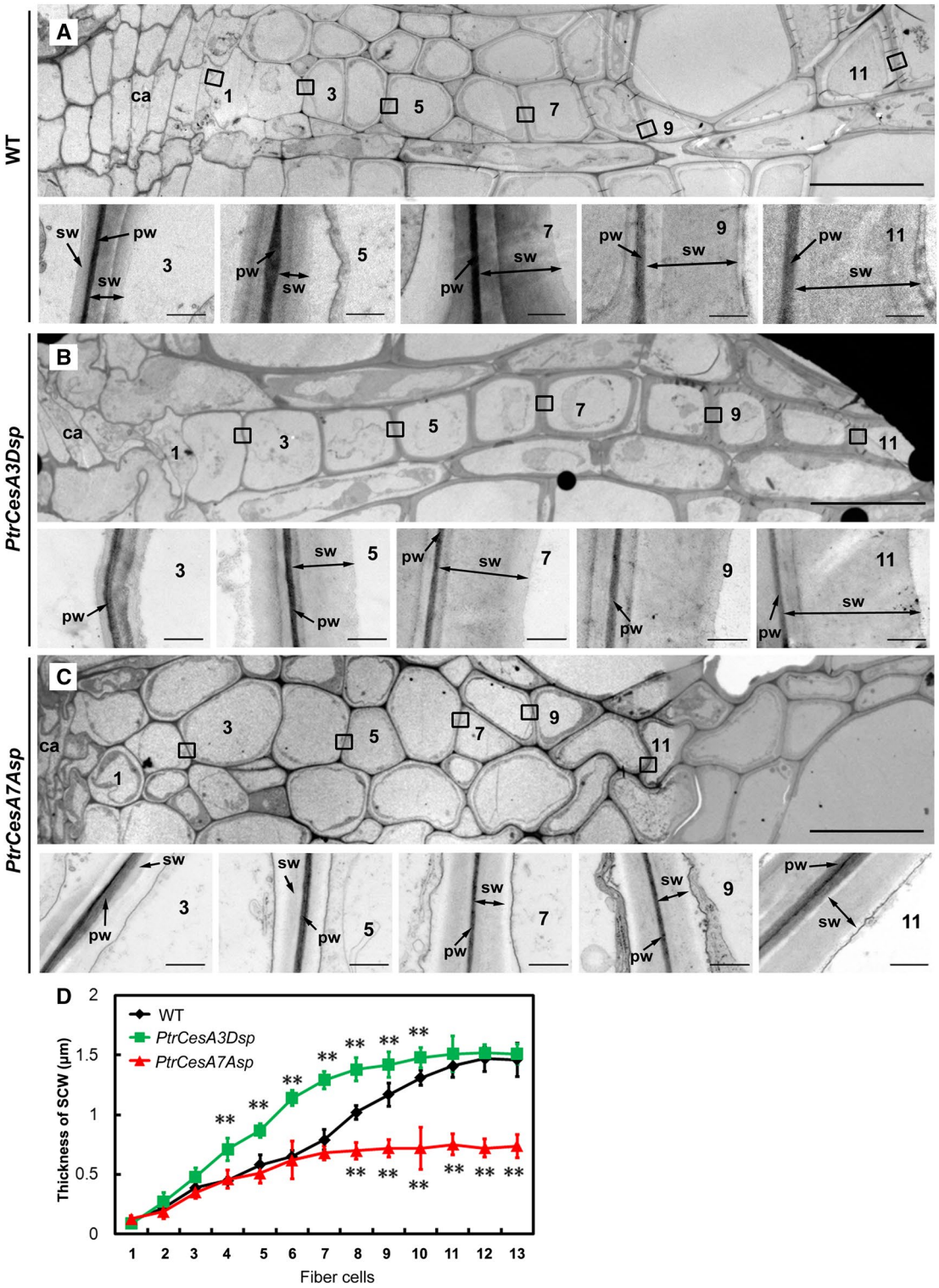

Fig. 3 Suppression of *PtrCesA7A* and *PtrCesA3D* affected secondary cell wall thickening. **a** Cell wall thickening was recorded in a file of fiber cells using a transmission electron microscope. Enlargements of the secondary cell wall structure show that the first layer formed in the 1st–2nd cells, the second layer formed in 3rd–8th cells and the third layer formed in ninth to eleventh cells. **b** The Secondary wall thickening in *PtrCesA3D* suppression. **c** The Secondary wall thickening in *PtrCesA7A* suppression. **d** Cell wall thickness in a file of fiber cells. Twenty cells in each position from 5 biological repeats in wild-type and transgenic plants were measured. Significance as determined by Student's *t* test. The values are means ± SE. $^{**}P < 0.01$. *Bars* 20 μm in cell files, 0.5 μm in wall structure enlargements. *sw* secondary cell wall, *pw* primary cell wall, *ca* cambium, *WT* wild-type plants, *sw* secondary cell wall, *pw* primary cell wall, *ca* cambium

of the secondary wall started in the 1st–2nd cells. The secondary cell wall with a two-layer structure was seen in the 3rd–4th cells and with a three-layer structure in the 9th to 12th cells (Fig. 3a). Suppression of *PtrCesA3D* and *PtrCesA7A* expression had different effects on the wall-thickening process. In a fiber file from the 3rd to 10th cells, *PtrCesA3D* suppression enhanced wall-thickening in the early thickening stage. While in the matured fiber cell (the 12th cell in a fiber file), *PtrCesA3D*-suppressed plants displayed a similar fiber cell wall thickness as that of the wild-type plant (Fig. 3b, d). On the other hand, *PtrCesA7A* suppression, which did not affect wall thickness at the early stage (from the 1st–6th cell in a fiber file), caused the wall thickening ceased at the 7th cell (Fig. 3c, d), which still underwent strong wall-thickening in the wild-type (Fig. 3a, d). The wall thickness of the matured fiber cell (the 12th cell in a fiber file) in *PtrCesA7A*-suppressed plants was only half of that in wild type. The wall was deformed in some of the xylem cells (Fig. 3b, c). The multilaminar wall structure was also affected in the *CesA* suppressed plants. Compared to the three-layer fiber wall structure in wild-type plants, a two-layer structure in *PtrCesA3D*-suppressed plant (Fig. 3b) and one layer structure in *PtrCesA7A*-suppressed plant (Fig. 3c) were observed. These results indicate that suppression of *PtrCesA3D* and *PtrCesA7A* expression led to different secondary cell wall thickening in xylem fiber cells, which might be attributed to the different roles that different type *CesA* genes play in formation of the multilaminar secondary cell wall structure.

Suppression of *PtrCesA3D* and *PtrCesA7A* affected cellulose accumulation and degradation

To investigate the two type *CesA* effect on wood cell wall composition, the chemical composition in wood was analyzed. Holocellulose content was dramatically reduced in *PtrCesA7A*-suppressed plants compared to a slight reduction in *PtrCesA3D*-suppressed plants (Fig. 4a). Lignin content increased in both *PtrCesA3D* and *PtrCesA7A*-suppressed plants (Fig. 4b), though *PtrCesA7A* suppressed plants showed relatively higher lignin content compared to *PtrCesA3D* suppressed plants (Fig. 4b). Interestingly, chemical examination showed that crystalline cellulose content, as calculated by the Updegraff method, was

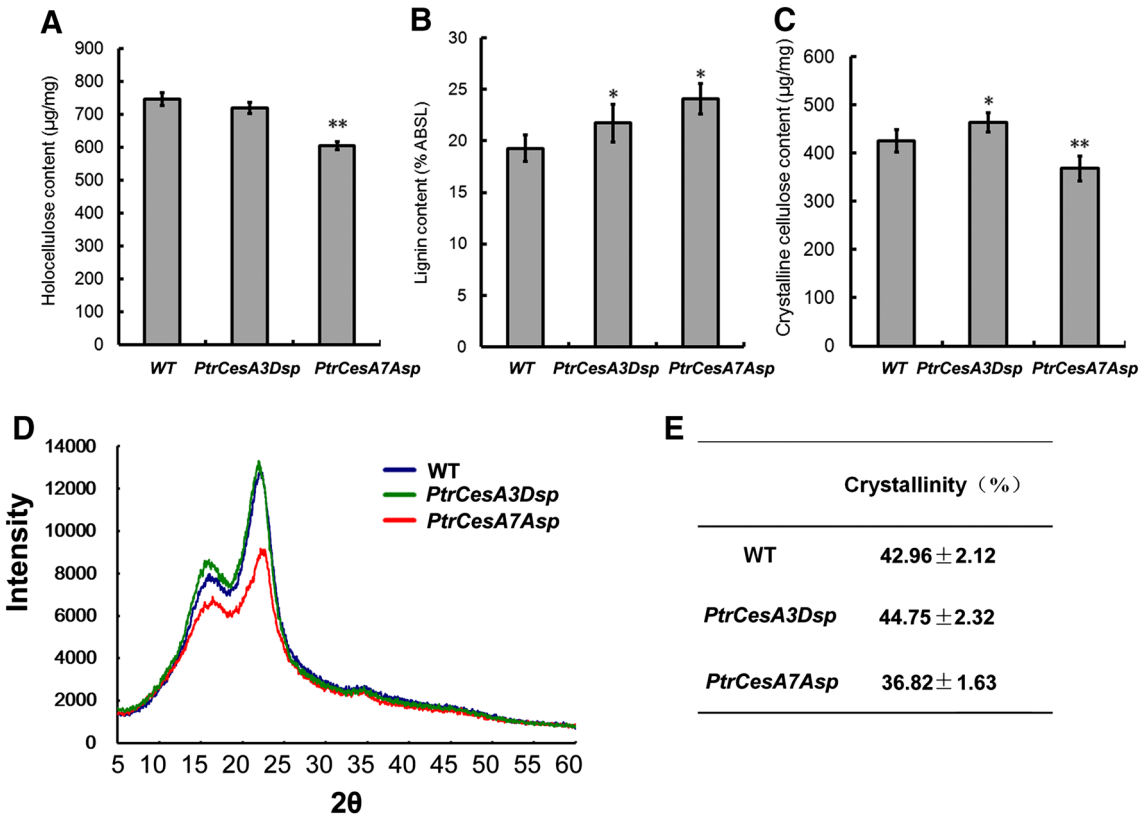

Fig. 4 Suppression of *PtrCesA7A* and *PtrCesA3D* affects cellulose content and crystallinity. **a** Holocellulose content, **b** ABSL (acetyl bromide soluble lignin) lignin content, and **c** crystalline cellulose content. **d** X-ray diffraction (XRD) analysis of cellulose crystallites and **e** cellulose crystallinity index calculated from XRD. Significance as determined by Student's t-test. The values are means ± SE. Biological repeats n = 5. **P < 0.01, *P < 0.05. *WT* wild-type plants

increased in *PtrCesA3D*-suppressed plants but reduced in *PtrCesA7A*-suppressed plants (Fig. 4c). X-ray diffraction measurement further confirmed this cellulose crystallinity changes in the transgenic plants (Fig. 4d, e). Suppression of the *PtrCesA3D* and *PtrCesA7A* expression also affected monosaccharide composition in hemicelluloses (Table 1). Xylose and mannose content, which are the major monosaccharides in the secondary cell wall hemicelluloses (xylan and mannan), significantly decreased in *PtrCesA7A*-suppressed plants but slightly increased in *PtrCesA3D*-suppressed plants. Other monosaccharides, including glucose, arabinose, galactose were little changed. The changes in monosaccharide composition suggest that interruption of the cellulose biosynthesis during wall-thickening affected accumulation of the secondary cell wall hemicelluloses. Cellulose digestibility by cellulase was also analyzed. Wood cell wall samples were pretreated and digested by cellulase. Measurement of the glucose release efficiency indicates that *PtrCesA7A* suppression led to higher cellulose digestibility while *PtrCesA3D* suppression resulted in lower cellulose digestibility compared to the wild-type (Fig. 5). However, it remains to be further investigated whether this cellulose digestibility change is related to the lower crystalline cellulose content in *PtrCesA7A*-suppressed plants and higher crystalline cellulose content in *PtrCesA3D*-suppressed plants.

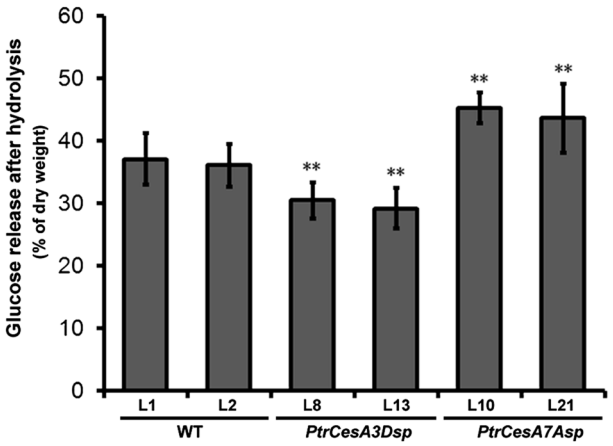

Fig. 5 Cellulose digestibility of wood cell walls. Significance as determined by Student's *t* test. The values are means ± SE. Biological repeats n = 5. **P < 0.01, *WT* wild-type plants

Discussion

In wood formation, a large amount of cellulose is synthesized and deposited as cellulose microfibrils in wood secondary cell walls. Cellulose is known to display different characteristics in the multilaminar secondary wall structure of wood (Evert 2006). Our previous study isolated two type CSCs from *Populus* differentiating xylem tissue undergoing multilaminar secondary cell wall formation (Song et al. 2010). Here we report an array of new evidence for understanding the function of two type CSC *CesA* genes in the process of wood secondary cell wall thickening.

Two type CSC *CesA* genes are differentially expressed in the process of multilaminar secondary wall formation

A family of *CesA* genes is found in each of the sequenced plant genomes. In *Arabidopsis, CesA* genes are divided into two types as primary cell wall *CesA*s and secondary cell wall *CesA*s. It is believed that two type CesAs form different CSCs which showed different moving velocity on the plasma membrane (Watanabe et al. 2015). On the basis of sequence homology, *CesA* genes from other species are also classified as primary and secondary cell wall *CesA*s. However, recent studies showed that the primary cell wall *CesA* can function in secondary cell wall biosynthesis and the secondary cell wall *CesA* can also function in primary cell wall biosynthesis (Carroll et al. 2012). During secondary wall thickening in *Populus, PtrCesA* genes classified as both primary and secondary cell wall *CesA*s are actively expressed (Suzuki et al. 2006; Song et al. 2010). The two type CSCs were found to be present during wood secondary wall formation. In the process of fiber cell wall thickening, the two type CSC genes displayed different expression pattern. One type CSC *CesA* expression was increased significantly along with the wall-thickening process, while the

Table 1 Monosaccharide composition of hemicelluloses in wood tissue

Plants	Xyl	Ara	Glc	Gal	Man
WT	247.56 ± 7.19	12.85 ± 0.12	12.96 ± 0.54	6.95 ± 1.52	17.85 ± 2.80
PtrCesA3Dsp	252.01 ± 9.54**	12.27 ± 0.22	12.70 ± 0.64	6.85 ± 1.09	20.52 ± 3.13*
PtrCesA7Asp	176.80 ± 1.61**	14.68 ± 0.63	13.19 ± 0.42	7.08 ± 2.00	13.06 ± 2.97*

WT wild-type plants, *Xyl* xylose, *Ara* arabinose, *Glc* glucose, *Gal* galactose, *Man* mannose. The values are calculated by Mol% in AIR. Values are means ± SE, n = 5. Significance as determined by Student's *t* test *P < 0.05, **P < 0.01

other type CSC *CesA* expression was gradually decreased. This suggests that two type CSC *CesA*s are involved in the fiber cell wall-thickening process through different manners. A number of studies have also reported that primary cell wall *CesA* genes also participated in secondary wall formation in *Arabidopsis*. For example, primary wall *CesA* genes are detected in support of cellulose synthesis during secondary wall thickening of *Arabidopsis* shoot trichomes and cotton fibers (Betancur et al. 2010). *CesA9*, considered a primary cell wall *CesA* gene, is found to play a role in the secondary cell wall biosynthesis in radial cell walls of epidermal seed coats (Stork 2010). These findings raise a possibility that *CesA* genes that are previously classified according to their association with primary and secondary cell wall formation may jointly function in cellulose biosynthesis during secondary cell wall formation.

CesA suppresssion affected the multilaminar structure of wood fiber cell walls

During wood formation, cellulose microfibrils produced by CSCs are deposited in the multilaminar structure (S1, S2 and S3) of wood secondary cell walls with different characters and orientations in different layers (Evert 2006; Brändström 2002). In this study we observed that two type *PtrCesA*s are involved in the wall-thickening process of xylem fiber cells in association with formation of the secondary cell wall laminar structure. Suppression of the two type *PtrCesA* genes displayed different effect on modifying the secondary cell wall thickening. Suppression of *PtrCesA7A*, homologous to *Arabidopsis* secondary cell wall *CesA*, significantly resulted in lower cellulose content and disrupted multilaminar structure of the fiber secondary cell wall. Alternatively, suppression of *PtrCesA3D*, homologous to *Arabidopsis* primary cell wall *CesA*, modified the formation of the fiber cell wall multilaminar structure. Although both suppressions resulted in changes in secondary cell walls, it is unclear whether suppression of the primary wall *CesA* homolog indirectly caused the secondary cell wall alterations. Nevertheless, the results suggest that formation of the wood cell wall laminar structure may be associated with the roles the two type CSC genes play in cellulose accumulation during xylem cell wall thickening.

CSCs may play a role in regulating cellulose structural characters

Cellulose displays a variety of structural characters, including crystallinity, DP, and microfibril orientation in multilaminar structures of wood secondary cell walls (OSullivan 1997; Sjöström 1993). Cellulose crystallization occurs when the cellulose glucan chains were transported out from the CSC pores on the plasma membrane (Morgan et al. 2013). It is hypothesized that CSCs coordinate the process of polymerization and crystallization by helping to assemble glucan chains into microfibril (OSullivan 1997; Somerville 2006; Herth 1983). Several factors, such as CSC structure, COBRA family members, microtubule organization (Harris et al. 2012; Liu et al. 2013; Fujita et al. 2011; Li et al. 2015), have been studied for their role affecting the cellulose characters deposited in *Arabidopsis* cell walls. In *Populus*, silencing of *CesA8* gene dramatically reduced cellulose content and crystallinity in wood (Joshi et al. 2011), and mutation to residues AtCesA1^{A903V} and AtCesA3^{T942I} in the C-terminal transmembrane region reduced crystalline cellulose content and increased the velocity of CSCs (Harris et al. 2012), suggesting the possibility that the CSC itself plays a role in cellulose crystallization. In this study, *PtrCesA7A* and *PtrCesA3D*, representing two type CSC *CesA* genes displayed different effect on formation of crystalline cellulose in wood tissue. In consistent with this, cellulose with different characters, such as crystallinity is deposited in *Arabidopsis* primary cell wall and secondary cell walls, in which two different type CSCs have been characterized (Buchanan et al. 2000; Desprez et al. 2007; Atanassov et al. 2009; McFarlane et al. 2014). Although the mechanisms underlying the cellulose deposition with different character structures have not been fully elucidated, this study provides a clue to aid in understanding the CSC role in formation of cellulose structural characters and multilaminar wall structures during wood cell wall thickening.

Materials and methods

Plant material and growth condition

Populus×*euramericana* cv. '*Nanlin895*' was used for genetic transformation and analysis. Young *Populus* trees were grown in a phytotron with a light and dark cycle of 16 and 8 h at 22 °C or grown in a greenhouse as described (Song et al. 2014).

CesA expression analysis

To analyze *CesA* gene expression during secondary cell wall thickening, the 16th–18th internodes of *Populus* trees were sectioned and fixed according to a previously used protocol (Song et al. 2010). The wall-thickening cells were collected using a laser microdissection system and total RNA was extracted using a PicoPure RNA isolation kit (Arcturus Bioscience). After amplification, RNA was reversely transcribed into cDNAs which were then used for gene expression analysis as described (Song et al. 2010).

Gene-specific primers were designed to amplify a specific fragment of *CesA* genes (Table S1) and quantitative

real-time PCR was performed using SYBR® Green Master Mix on a MyiQ Real-Time PCR Detection System (Bio-Rad, Winston-Salem, NC, USA). The PCR program was set as follow: 94 °C for 10 min, 42 cycles of 94 °C for 15 s, 57 °C for 15 s and 72 °C for 15 s. Dissociation curve was analyzed to confirm the generation of a single and specific product in each reaction. Relative gene expression was determined by a ΔCT method, with *PtrActin2* as an internal control. All reactions were performed with three biological repeats, and three technical repeats were performed for each primer.

To further analyze *CesA* expression in field grown trees, two stages of cell wall thickening samples were collected from 5-year-old trees at a growth season by skinning the developing xylem tissue into two layers (~0.5 mm thickness per layer). The collected tissue was immediately frozen and stored in liquid nitrogen for gene expression and protein analysis. 500 ng of total RNA was reversely transcribed into cDNAs for gene expression analysis. For CesA protein analysis, the collected xylem tissue was ground into a fine powder and protein extraction was carried out as described (Song et al. 2010). CesAs were analyzed by Western blot using antibodies (1 μg μl^{-1}) of anti-CesA7 (recognizing PtrCesA7A and PtrCesA7B), anti-CesA8 (recognizing PtrCesA8A and PtrCesA8B), anti-CesA1(recognizing PtrCesA1A and PtrCesA1B), and anti-CesA3 (recognizing PtrCesA3C and PtrCesA3D) (Song et al. 2010) for CesA detection.

For identification of CSCs in developing xylem, CSCs were isolated from xylem microsomal fraction according to our established immuno-pull-down procedure (Song et al. 2010). Isolated CSCs (50 μg/lane) were firstly subjected to electrophoresis separation at 4 °C using a blue native gradient PAGE gel (4–15%). Then, the first dimension gel was cut into strips along the sample lanes of electrophoresis and treated in 50 mM Tris–HCl, pH 7.5, 2% (w/v) SDS, 50 mM DTT for 30 min at room temperature. Then the strips were overlaid on a SDS–PAGE gel for second dimension separation. Separated proteins were transferred onto a PVDF membrane and subjected to immunoblot detection using CesA antibodies.

RNA interference vector construction and plant transformation

The nucleic acid sequences which cover an HVR region of *CesA7A* and *CesA3D* genes were amplified (See Table S1 for amplification primers) and inserted into a pRNAi vector (Limpens et al. 2004), respectively. The RNAi cassette under control of a caulilower mosaic virus 35 S promoter was removed into pCambia2300 binary vector and then transformed into plants using an *Agrobacterium*-mediated method according to the protocol used in our laboratory (Li et al. 2003).

Measurement of mechanical strength

Stems of 6-month-old *Populus* trees in a greenhouse were prepared for a mechanical test according to our previous protocol (Yu et al. 2013). *Populus* stems with an average diameter of 1 cm were subjected for bending test using a mechanical testing machine (HY-0580, http://www.hengyi-yiqi.com). Mechanical strength was calculated using the modulus of rupture (MOR) in bending according to a described method (Kern et al. 2005).

Electron microscopic analysis of secondary cell wall thickening

The 12th internode (counting from above) of *Populus* stem was cut into 2–3 mm in length and fixed in 2.5% glutaraldehyde in PBS (0.1 M, pH 7.4). After vacuum infiltration, the fixed stem was set at 4 °C overnight. Then fixed tissue was washed with 0.1 M PBS and immerged in 0.5% osmic acid for 2 h. After three washes with 0.1 M PBS, the tissue was dehydrated in an ethanol series (final concentration of 80% ethanol), and embedded in LR white resin (Polysciences, Warrington, PA, USA). After polymerization at 50 °C for overnight, the resin-embedded sample was sectioned into 60 nm-thick and mounted on gold mesh grids. After dried at room temperature, sample section was sequentially stained using uranylacetate and lead citrate. The stained section was observed under an electron microscope (H-7650; HITACHI, Kyoto, Japan) at 80 kV and cell wall thickness was measured by the Image J software (http://rsbweb.nih.gov/ij/index.html).

Wood composition and cellulose hydrolysis assay

Wood of 1-year-old *Populus* trees was dried and ground into fine powder and alcohol insoluble residue (AIR) was prepared (Song et al. 2014). The holocellulose content was determined according to the method established in our laboratory (Hou and Li 2011). Lignin content was determined as described (Foster et al. 2010a). Crystalline cellulose content and monosaccharide composition were determined according to the (Foster et al. 2010b) method with minor modifications. Briefly, a total of 2 mg AIR was hydrolyzed by 250 μl of 2 M trifluoroacetic acid (TFA,) at 121 °C for 90 min. The supernatant was dried in a rotatory evaporator and subjected to alditol acetate derivatization and acetylation for monosaccharide analysis. Monosaccharides were detected and quantified using a GC-MS system equipped with an SP-2380 capillary column (Agilent 5975 inert MSD system). The

residues were used for crystalline cellulose assay using an anthrone sulfuric acid method (Foster et al. 2010b). Briefly, the residue was treated with 1 ml updegraff reagent (Acetic acid: nitric acid: water, 8:1:2) to remove non-crystalline cellulose. The remaining residue was hydrolyzed by 175 µl of 72% sulfuric acid at room temperature for 60 min. After hydrolysis, the released glucose was subjected to anthrone assay for assessment of crystalline cellulose content.

Cellulose hydrolysis was analyzed according to our previously established protocol (Hou and Li 2011). Briefly, wood mill passed through a 60-mesh screen was collected. 0.5 g wood mill was treated with 10 ml 4% sulfuric acid. After reaction at 121 °C for 1 h in an autoclave, reaction residue was separated by centrifugation, washed three times and suspended in 25 mL of 0.1 M sodium citrate buffer at pH 4.8. Then the suspended residue was hydrolyzed by adding 100 filter paper units (FPU) cellulase (E.C. 3.2.1.4) (Yakult Honsha, Tokyo, Janpan) at 50 °C for 48 h. Glucose concentration was measured by dinitrosalicylic acid (DNS) method using glucose as a standard.

X-ray diffraction (XRD) analysis of wood cellulose

Wood mill was passed through an 80-mesh screen and analyzed for cellulose crystallinity using an X-ray diffraction meter (D/Max-2550 PC, Rigaku, Japan). The X-ray generator equipped with a copper tube was operated at 40 kV and 30 mA. Wood sample was irradiated with a CuKα radiation with a wavelength of 0.154 nm. XRD spectra were acquired over a 2θ range of 5°–60° at 0.02° intervals. Measurement was carried out with 2 s per 2θ intervals at room temperature with three biological repeats. XRD crystallinity index (CI) was calculated according to intensity (I) height ratio: $CI = (I22° - I18°)/I22° \times 100\%$ using Segal method (Lionetto et al. 2012; Segal et al. 1959).

Acknowledgements We thank Xiaoyan Gao, Zhiping Zhang and Jiqin Li assistance for electron microscopic observation, Wenli Hu for GC–MS analysis. This work was financially supported by the National Natural Science Foundation of China (31130012, 31300500) and the Ministry of Science and Technology of China (2012CB114502).

Compliance with ethical standards

Conflict of interest The authors declare that they have no conflict of interest.

Author contributions WX and DS carried out the experiments, contributing equally to this work, JYS performed transformation and grew *Populus* trees, JHS carried out part of the experiments. WX, DS and LL designed the study, analyzed the data and wrote the manuscript. All authors have read and approved the final manuscript.

References

Arioli T, Peng L, Betzner AS, Burn J, Wittke W, Herth W, Camilleri C, Hofte H, Plazinski J, Birch R, Cork A, Glover J, Redmond J, Williamson RE (1998) Molecular analysis of cellulose biosynthesis in Arabidopsis. Science 279(5351):717–720

Atanassov II, Pittman JK, Turner SR (2009) Elucidating the mechanisms of assembly and subunit interaction of the cellulose synthase complex of Arabidopsis secondary cell walls. J Biol Chem 284(6):3833–3841

Betancur L, Singh B, Rapp RA, Wendel JF, Marks MD, Roberts AW, Haigler CH (2010) Phylogenetically distinct cellulose synthase genes support secondary wall thickening in Arabidopsis shoot trichomes and cotton fiber. J Integr Plant Biol 52(2):205–220

Blaschek W, Koehler H, Semler U, Franz G (1982) Molecular weight distribution of cellulose in primary cell walls. Planta 154(6):550–555

Brändström J (2002) Morphology of Norway spruce tracheids with emphasis on cell wall organisation, vol 237. Swedish University of Agricultural Sciences Uppsala, Sweden

Buchanan BB, Gruissem W, Jones RL (2000) Biochemistry and molecular biology of plants, vol 3. American Society of Plant Physiologists, Rockville

Carroll A, Mansoori N, Li SD, Lei L, Vernhettes S, Visser RGF, Somerville C, Gu Y, Trindade LM (2012) Complexes with mixed primary and secondary cellulose synthases are functional in Arabidopsis plants. Plant Physiol 160(2):726–737. doi:10.1104/pp.112.199208

Delmer DP (1999) CELLULOSE BIOSYNTHESIS: exciting times for a difficult field of study. Annu Rev Plant Physiol Plant Mol Biol 50:245–276

Desprez T, Juraniec M, Crowell EF, Jouy H, Pochylova Z, Parcy F, Hofte H, Gonneau M, Vernhettes S (2007) Organization of cellulose synthase complexes involved in primary cell wall synthesis in *Arabidopsis thaliana*. Proc Natl Acad Sci USA 104(39):15572–15577

Doblin MS, Kurek I, Jacob-Wilk D, Delmer DP (2002) Cellulose biosynthesis in plants: from genes to rosettes. Plant Cell Physiol 43(12):1407–1420

Evert RF (2006) Esau's Plant anatomy: meristems, cells, and tissues of the plant body: their structure, function, and development. 3rd edn Wiley, New Jersey

Foster CE, Martin TM, Pauly M (2010a) Comprehensive compositional analysis of plant cell walls (lignocellulosic biomass) part I: Lignin. J Vis Exp (37):e1745. doi:10.3791/1745

Foster CE, Martin TM, Pauly M (2010b) Comprehensive compositional analysis of plant cell walls (lignocellulosic biomass) part II: carbohydrates. J Vis Exp (37):e1837. doi:10.3791/1837

Fujita M, Himmelspach R, Hocart CH, Williamson RE, Mansfield SD, Wasteneys GO (2011) Cortical microtubules optimize cell-wall crystallinity to drive unidirectional growth in Arabidopsis. Plant J 66(6):915–928

Harris DM, Corbin K, Wang T, Gutierrez R, Bertolo AL, Petti C, Smilgies DM, Estevez JM, Bonetta D, Urbanowicz BR, Ehrhardt DW, Somerville CR, Rose JKC, Hong M, DeBolt S (2012) Cellulose microfibril crystallinity is reduced by mutating C-terminal transmembrane region residues CESA1(A903V) and CESA3(T942I) of cellulose synthase. Proc Natl Acad Sci USA 109(11):4098–4103

Herth W (1983) Arrays of plasma-membrane rosettes involved in cellulose microfibril formation of spirogyra. Planta 159(4):347–356

Hill JL, Hammudi MB, Tien M (2014) The Arabidopsis cellulose synthase complex: a proposed hexamer of CESA trimers in an equimolar stoichiometry. Plant Cell 26(12):4834–4842

Hou S, Li L (2011) Rapid characterization of woody biomass digestibility and chemical composition using near infrared spectroscopy. J Integr Plant Biol 53(2):166–175

Joshi CP, Thammannagowda S, Fujino T, Gou JQ, Avci U, Haigler CH, McDonnell LM, Mansfield SD, Mengesha B, Carpita NC (2011) Perturbation of wood cellulose synthesis causes pleiotropic effects in transgenic aspen. Mol plant 4(2):331–345

Kern KA, Ewers FW, Telewski FW, Koehler L (2005) Mechanical perturbation affects conductivity, mechanical properties and aboveground biomass of hybrid poplars. Tree Physiol 25(10):1243–1251

Kimura S, Laosinchai W, Itoh T, Cui X, Linder CR, Brown RM Jr (1999) Immunogold labeling of rosette terminal cellulose-synthesizing complexes in the vascular plant vigna angularis. Plant Cell 11(11):2075–2086

Li L, Zhou Y, Cheng X, Sun J, Marita JM, Ralph J, Chiang VL (2003) Combinatorial modification of multiple lignin traits in trees through multigene cotransformation. Proc Natl Acad Sci USA 100(8):4939–4944

Li S, Lei L, Yingling YG, Gu Y (2015) Microtubules and cellulose biosynthesis: the emergence of new players. Curr Opin Plant Biol 28:76–82

Limpens E, Ramos J, Franken C, Raz V, Compaan B, Franssen H, Bisseling T, Geurts R (2004) RNA interference in Agrobacterium rhizogenes-transformed roots of Arabidopsis and Medicago truncatula. J Exp Bot 55(399):983

Lionetto F, Del Sole R, Cannoletta D, Vasapollo G, Maffezzoli A (2012) Monitoring Wood Degradation during Weathering by Cellulose Crystallinity. Materials 5(10):1910–1922

Liu LF, Shang-Guan KK, Zhang BC, Liu XL, Yan MX, Zhang LJ, Shi YY, Zhang M, Qian Q, Li JY, Zhou YH (2013) Brittle culm1, a COBRA-Like protein, functions in cellulose assembly through binding cellulose microfibrils. PLoS Genet 9(8)

McFarlane HE, Doring A, Persson S (2014) The cell biology of cellulose synthesis. Annu Rev Plant Biol 65:69–94

Mellerowicz EJ, Sundberg B (2008) Wood cell walls: biosynthesis, developmental dynamics and their implications for wood properties. Curr Opin Plant Biol 11(3):293–300

Morgan JL, Strumillo J, Zimmer J (2013) Crystallographic snapshot of cellulose synthesis and membrane translocation. Nature 493(7431):181–186

Müller M, Burghammer M, Sugiyama J (2006) Direct investigation of the structural properties of tension wood cellulose microfibrils using microbeam X-ray fibre diffraction. Holzforschung 60(5):474–479

Mutwil M, Debolt S, Persson S (2008) Cellulose synthesis: a complex complex. Curr Opin Plant Biol 11(3):252–257

OSullivan AC (1997) Cellulose: the structure slowly unravels. Cellulose 4(3):173–207

Persson S, Paredez A, Carroll A, Palsdottir H, Doblin M, Poindexter P, Khitrov N, Auer M, Somerville CR (2007) Genetic evidence for three unique components in primary cell-wall cellulose synthase complexes in Arabidopsis. Proc Natl Acad Sci USA 104(39):15566–15571

Saxena IM, Brown RM Jr (2005) Cellulose biosynthesis: current views and evolving concepts. Ann Bot 96(1):9–21

Segal L, Creely J, Martin A, Conrad C (1959) An empirical method for estimating the degree of crystallinity of native cellulose using the X-ray diffractometer. Text Res J 29(10):786–794

Sjöström E (1993) Wood chemistry: fundamentals and applications, 2nd edn. Academic press, San Diego

Somerville C (2006) Cellulose synthesis in higher plants. Annu Rev Cell Dev Biol 22:53–78

Song D, Shen J, Li L (2010) Characterization of cellulose synthase complexes in Populus xylem differentiation. New Phytol 187:777–790

Song D, Sun J, Li L (2014) Diverse roles of PtrDUF579 proteins in Populus and PtrDUF579-1 function in vascular cambium proliferation during secondary growth. Plant Mol Biol 85:601–602

Stork J, Harris D, Griffiths J, Williams B, Beisson F, Li-Beisson Y, Mendu V, Haughn G, Debolt S (2010) CELLULOSE SYNTHASE9 serves a nonredundant role in secondary cell wall synthesis in Arabidopsis epidermal testa cells. Plant Physiol 153(2):580–589

Suzuki S, Li L, Sun YH, Chiang VL (2006) The cellulose synthase gene superfamily and biochemical functions of xylem-specific cellulose synthase-like genes in Populus trichocarpa. Plant Physiol 142(3):1233–1245

Taylor NG, Scheible WR, Cutler S, Somerville CR, Turner SR (1999) The irregular xylem3 locus of Arabidopsis encodes a cellulose synthase required for secondary cell wall synthesis. Plant Cell 11(5):769–780

Taylor NG, Laurie S, Turner SR (2000) Multiple cellulose synthase catalytic subunits are required for cellulose synthesis in Arabidopsis. Plant Cell 12(12):2529–2540

Taylor NG, Howells RM, Huttly AK, Vickers K, Turner SR (2003) Interactions among three distinct CesA proteins essential for cellulose synthesis. Proc Natl Acad Sci U S A 100(3):1450–1455

Wang T, Hong M (2016) Solid-state NMR investigations of cellulose structure and interactions with matrix polysaccharides in plant primary cell walls. J Exp Bot 67(2):503–514

Wang J, Elliott JE, Williamson RE (2008) Features of the primary wall CESA complex in wild type and cellulose-deficient mutants of Arabidopsis thaliana. J Exp Bot 59(10):2627–2637. doi:10.1093/Jxb/Ern125

Washusen R, Evans R (2001) The association between cellulose crystallite width and tension wood occurrence in Eucalyptus globulus. IAWA J 22(3):235–244

Watanabe Y, Meents MJ, McDonnell LM, Barkwill S, Sampathkumar A, Cartwright HN, Demura T, Ehrhardt DW, Samuels AL, Mansfield SD (2015) Visualization of cellulose synthases in Arabidopsis secondary cell walls. Science 350(6257):198–203

Yu L, Sun J, Li L (2013) PtrCel9A6, an endo-1, 4-β-glucanase, is required for cell wall formation during xylem differentiation in Populus. Mol plant 6(6):1904–1917

Zhong R, Morrison WH 3rd, Freshour GD, Hahn MG, Ye ZH (2003) Expression of a mutant form of cellulose synthase AtCesA7 causes dominant negative effect on cellulose biosynthesis. Plant Physiol 132(2):786–795